

# Effect of particle shape on bulk-stress-strain relations of granular materials

Hans-Georg Mattutis, University of Electro-Communications, Department of Mechanical and Control Engineering, Chofu, Chofugaoka 1-5-1, Tokyo 182-8585, Japan  
 Nobuyasu Ito, Department of Applied Physics, School of Engineering, The University of Tokyo, Bunkyo-ku, Tokyo 113, Japan  
 Alexander Schinner, GeNUA mbh, Räterstraße 26, 85551 Kirchheim, Germany

## Abstract

The effect of the particle shape on the bulk-stress-strain-relations for triaxial compression of granular media is investigated via the molecular dynamics method. It is found that crucial properties exhibited by experimental granular media cannot be reproduced by round particle simulations, but only by the use of elongated particles.

## 1 Introduction

The paradigm of statistical physics is to obtain the description of macroscopic phenomena as statistical effects of the microscopic compounds. In solid state physics, one is used to the fact that replacing on kind of atoms in a solid alters the macroscopic properties of the solid, e.g. doping improves electric conductivity in semiconductors, adding chromium and manganese increase the hardness of steel etc. "Round" noble gas atoms have low evaporation temperatures, whereas solids made from atoms with "rough" covalent bonds exhibit high stability. In the granular community, most particle simulations are still performed using round particles, the "particle shape" as a material parameter is still widely neglected. In this paper, we want to show how the macroscopic stability is affected by the particle shape, and how the stability influences further properties of granular assemblies.

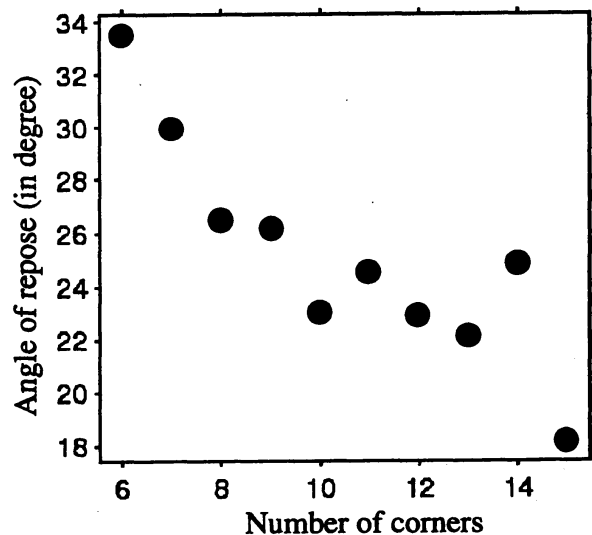


Figure 1: Angle of repose for a heap from mono-disperse particles with different numbers of corners. After [1].

## 2 Shape effects in granular research

In this section, give a brief overview about some established particle shape effects in granular materials.

## 2.1 Angle of repose

The angle of repose depends strongly on the shape of the particles, both experimentally and in simulations. Bricks with rectangular edges allow the easy building of vertical walls, nobody would choose bowling-ball shaped particles to obtain "high" angles of repose. Realistic angles of repose for granular materials are of the order of  $30^\circ$ , whereas spherical glass beads show critical angles of only about  $20^\circ$ . In Fig. 1, we have shown the dependence of the angle of repose for a heap from mono-disperse particles on the number of corners for non-elongated particles, i.e. polygons were inscribed into circles. Clearly, the angle of repose decreases with increasing number of corners.

## 2.2 Force networks

In two dimensions, compression under small strain for round particles leads to a force network which is characterized by a pattern where the large forces form a net with large meshes [2, 3]. The size of these meshes has been proposed to be the correlation length of granular media[4]. Nevertheless, for larger strains, or for elongated particles, such a mesh pattern is absent, and the large forces are contracted to chains[2]. The distribution also changes from a power-law like distribution[3] for the large forces to an exponential distribution, the investigation is in progress in connection with this article.

## 3 Triaxial Compression

The standard test of granular materials to derive their stress-strain curve is the triaxial compression, in which the compression along the  $z$ -axis occurs with constant velocity, whereas the pressure along the  $x$ - and  $y$ -axis is held constant. Experimentally, the sides of the granular medium are held by a rubber membrane, the constant pressure is realized by the constant pressure of a water reservoir on the rubber membranes, see Fig. 2.

### 3.1 Stress-Strain relations for experimental granular materials

A characteristic of the stress-strain relations for granular media under triaxial compression in contrast to e.g. uniaxial compression of metals is, that the stress curve has a clear

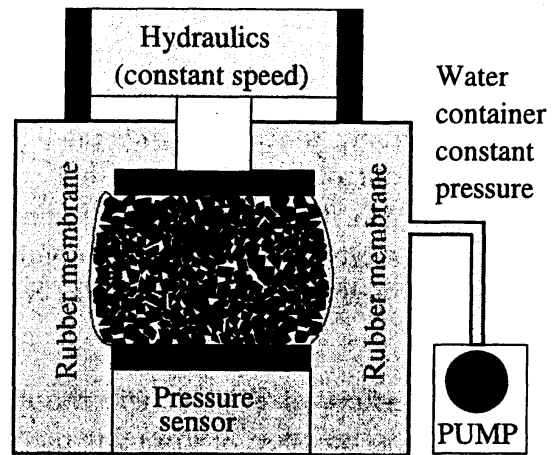
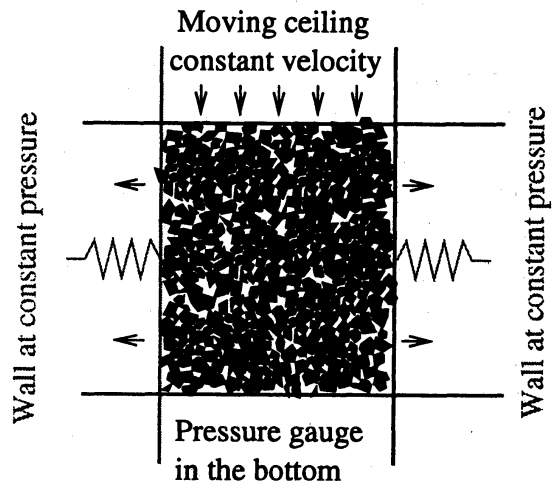


Figure 2: Schematic drawing for the experimental setup of triaxial-compression.



all walls without friction !  
Figure 3: Schematic drawing for the computational setup of triaxial-compression.

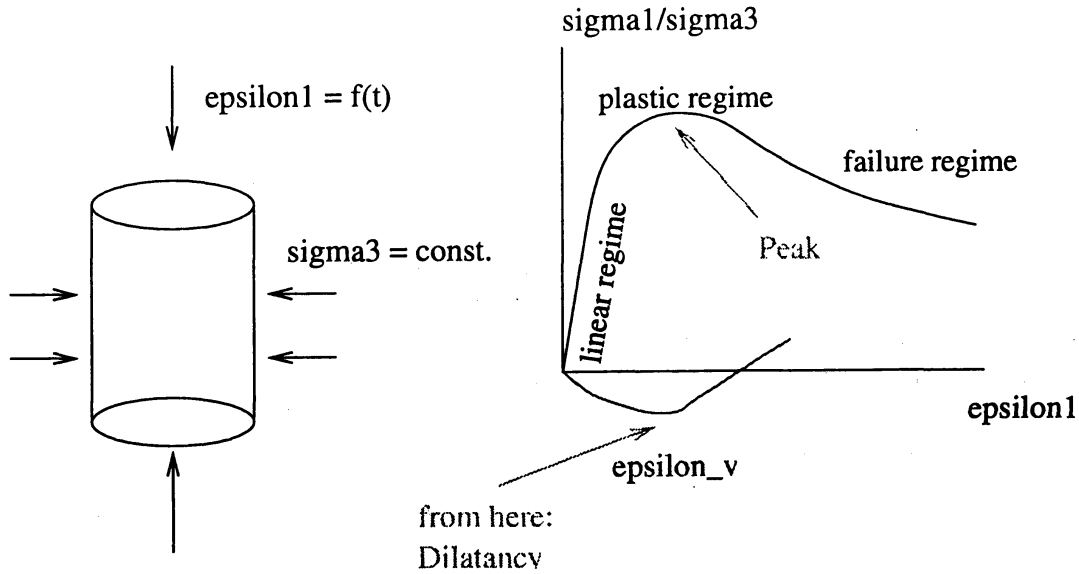


Figure 4: Schematic drawing for the triaxial compression (left) and the stress-strain curve for granular materials under triaxial compression (right), after [5]

maximum, where the material is in a plastic regime, for larger stresses the material enters the failure regime where the stress necessary to deform the material is smaller than the maximal yield stress, and the density-maximum/ minimum of the volume is not reached at the maximum stress, but before, due to Reynolds dilatancy, see Fig. 4.

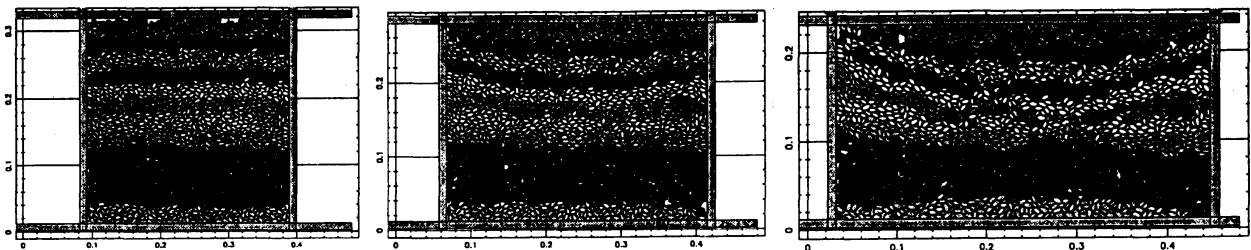


Figure 5: Initial, intermediate and final stage of a simulation run for triaxial compression with polygonal particles. The increase in the pore space due to Reynolds dilatancy during compression is clearly visible. One can see that the deformation of the sample volume is inhomogeneous.

### 3.2 Setup of the simulation

In our two dimensional simulation, triaxial compression reduces of course to biaxial compression, where the system is held under constant pressure along the x-axis and compressed under constant velocity along the y-axis. Because the simulation of the rubber membrane and the surrounding water would create an unnecessary overhead, we simulate the boundary of the axis which is not the compression axis via friction-less hard walls which are held by a non-linear spring which tries to keep the pressure constant, see Fig. 2. The modulus of elasticity of the particles was  $10^6$  N/m, the normal damping was chosen so that the two-particle collision was nearly “totally inelastic”. All simulations were

performed with the same normal dissipation. The coefficient for the Coulomb friction was chosen as 0.6 if not mentioned otherwise. The force models used for the ellipses are described in[6], for the polygons in[7]. The external pressure was kept at  $10^4$  N/m. A vertical stress of  $15 \cdot 10^4$  translates therefore into 15 times the horizontal stress. The volumes are given so that the volume at the beginning of the compression, when the upper lid gets in contact with the granular filling (left picture in Fig. 5), is normalized to 1. The particles used were either ellipses or polygons inscribed into ellipses with a varying number of corners. The proportion of the longer to the shorter half axis of the ellipses will be in the following be denoted as “elongation”. In the following, all strains are linear strains, the height of the volume is rescaled by the initial height.

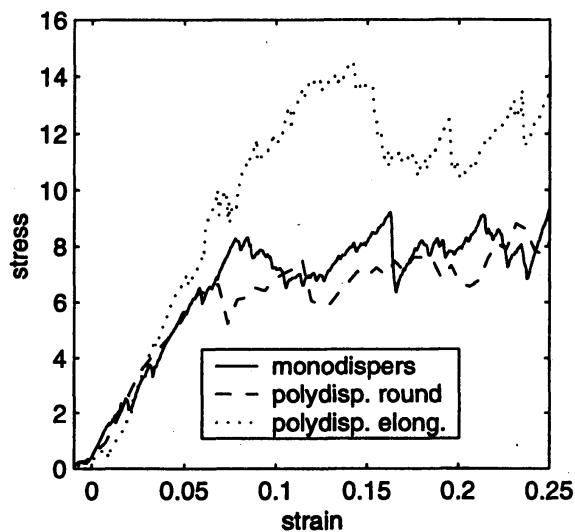


Figure 6: Stress-strain diagram for a single run of mono-disperse round particles (full line), polydisperse round particles (dashed line) and polydisperse elongated particles (dotted line), scaled by the external pressure.

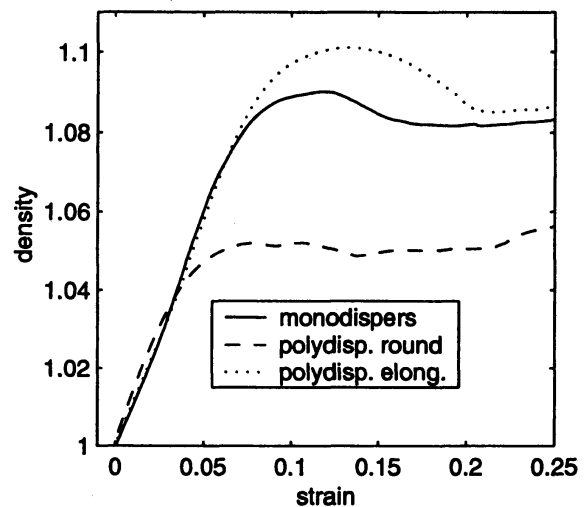


Figure 7: Density-strain diagram for the runs in Fig. 6 for mono-disperse round particles (full line), polydisperse round particles (dashed line) and polydisperse elongated particles (dotted line), scaled by the density before compression.

## 4 Stress-Strain relations

### 4.1 Results for single runs

For the sake of clarity, we will compare curves made for single runs of mono-disperse round particles, polydisperse round particles and polydisperse elongated particles. The stress-strain and density-strain relations for granular materials differ crucially depending on the shape of the particles. An aggregate of elongated particles with average elongation 1.8 can carry nearly twice as much stress as round polydisperse and mono-disperse particles, see Fig. 6. Moreover, the stress-strain distribution for “usual” granular media has a maximum, a criterion which is only fulfilled for elongated particles. For the density-strain-distribution, it is surprising that the maximal density for elongated polydisperse

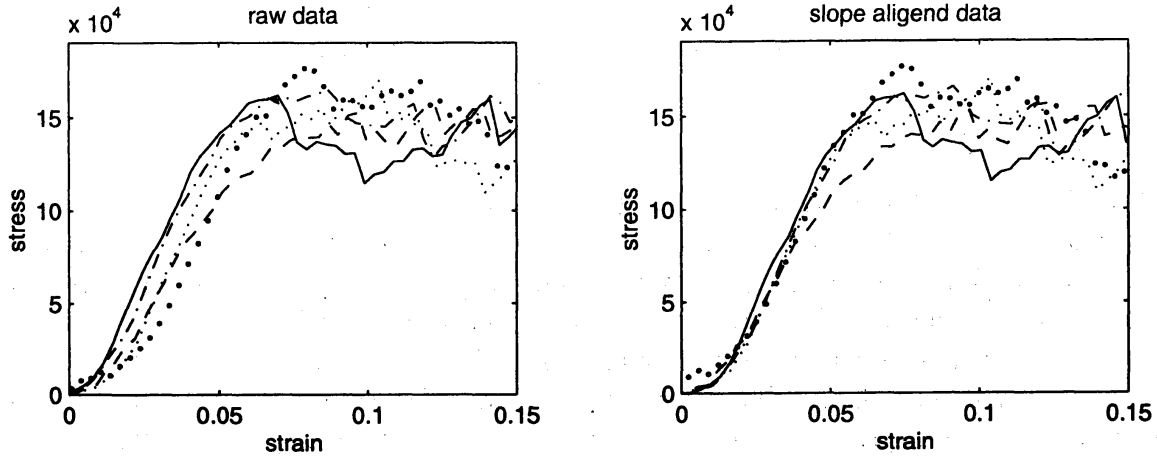


Figure 8: Raw data for four runs of stress-strain-curves (left) and the same data realigned along the slope (right) .

can be up to 5 % and for mono-disperse round particles up to 5 % higher than for polydisperse round particles. As can be seen in Fig. 6, if the compression of elongated particles is continued, the stresses rise again after the failure regime.

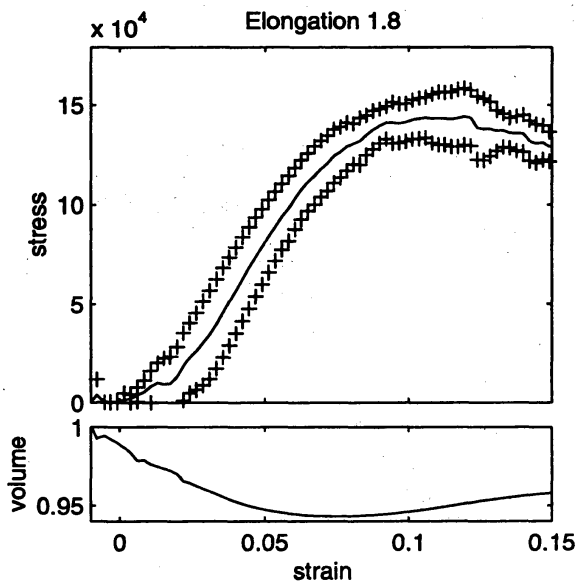


Figure 9: Stress-strain diagram for ellipses of average elongation 1.8.

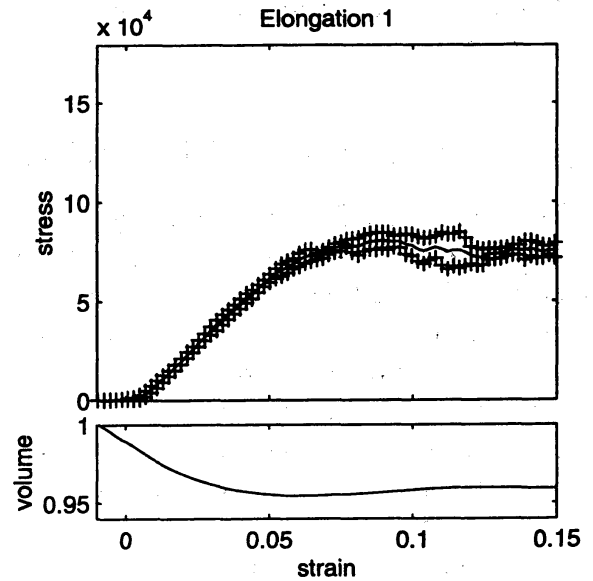


Figure 10: Stress-strain diagram for ellipses of average elongation 1.1.

## 4.2 The misery of averaging noisy curves

Especially two dimensions, the simulations data suffer from strong fluctuations. Averages of curves with relative maxima do not necessarily yield a curve with a maximum. Because the maximum of the single curves is of different size at different locations, the averaging may actually cancel out the maximum. To reduce this effect, we aligned the slope of the

stress-strain curves, see Fig. 8. In all following stress-strain diagrams, the statistic error bars of the 4 to 6 samples are indicated by +-signs in the graphs.

### 4.3 Elliptic particles

As for the single runs, the average maximal yield stress for ellipses (average elongation 1.8, Fig. 9) is nearly twice as large as for circles of the same size dispersion (Fig. 10). Compared to aggregates of elongated particles, aggregates of round particles have nearly only half the stability, as far as the yield stress is concerned, and also the relative maximum of the shear stress was conspicuously absent. The minimum for the volume of the cell (maximum of the density) is also markedly shallower for round than for elongated particles. One has to conclude that round particles do not exhibit proper behavior of granular materials in their stress-strain characteristics. We found that it was possible to manipulate the setup of the compression in such a way that a maximum in the stresses appeared by fixing one of the walls. Such a setup is definitely different from the true experimental setup.



Figure 11: “Elliptic-shaped” particles of elongation 1.8 with 7,14,32 and  $\infty$  number of corners

### 4.4 Roughness of the particles

Whereas the effect of the elongation turned out to be considerable, the effect of the roughness of the particles was not so crucial. Polygons have a “rougher” appearance than ellipses, and polygons with fewer corners look rougher than those with more corners. Fig. 12 shows the stress-strain diagram for polygons with 7 corners for the same average length- and size-distribution as for the ellipses in Fig.9. The only difference in the stress-strain relations of ellipses and polygons with 7 corners that the fluctuations are increased in the case of polygons, within the fluctuations, the position of the maximum and its numerical value is the same. This is rather surprising, because intuitively, one associates higher shear resistivity with rougher surfaces. It should be noted, that our investigation of “roughness” does not compare truly different surfaces, but particles with smooth surfaces, only a different number of corners. Using polygons instead of ellipses does not alter the macroscopic stress-strain behavior, and for truly modeling “micro-roughness”, using polygons with a few corners is not sufficient.

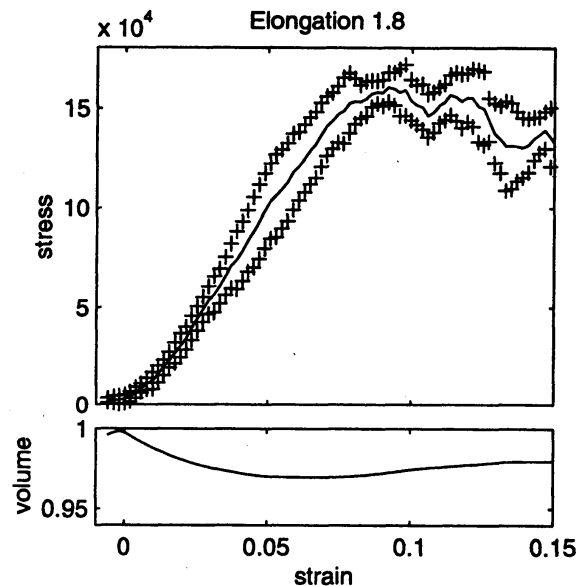


Figure 12: Stress-strain diagram for assemblies of polygonal particles of average elongation 1.8 and 7 corners.

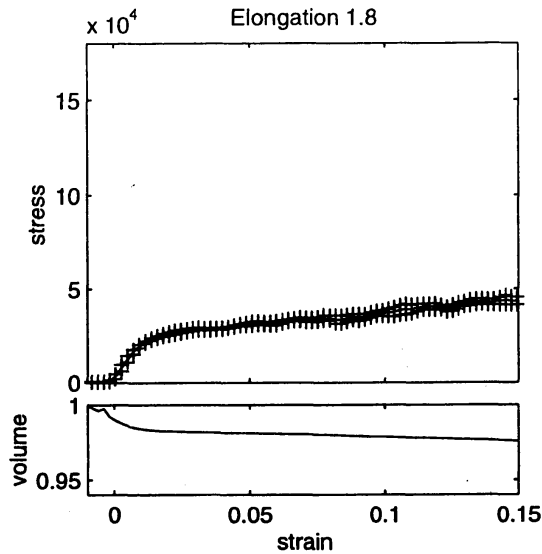


Figure 13: Stress-strain curve for particles with elongation 1.8 and vanishing Coulomb-friction.

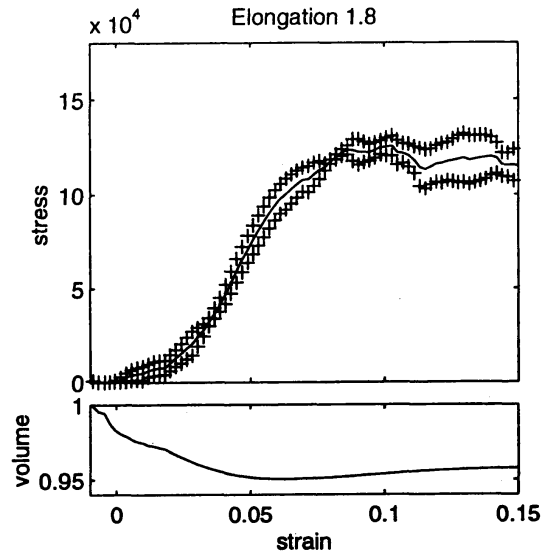


Figure 14: Stress-strain curve for particles with elongation 1.8 and Coulomb-friction coefficient 0.3.

#### 4.5 Friction effect

Ellipses with an elongation of 1.8 approximated by polygons with 32 corners with  $\mu = 0.0$  (left) and  $\mu = 0.3$  (right) show a definite deviation from the simulations with friction coefficient with  $\mu = 0.6$  in Fig. 12 and Fig. 9, though the size dispersion and the particle elongation were the same. For the friction coefficient  $\mu = 0.3$ , for the given average elongation of 1.8 the maximum in the shear stress which should be characteristic for granular media is hardly visible, and the corresponding relative minimum in the volume is only very weak. For the same size- and shape-distribution at vanishing friction coefficient  $\mu = 0.0$ , neither stress-strain nor stress-volume curves resemble those for typical for granular materials, and one has to conclude that simulations of granular materials at vanishing Coulomb friction do not really offer insights into realistic granular materials.

In this context, it is appropriate to ask where the transition between granular materials and liquids will occur if the size of the granular materials will be reduced, and at which length-scale the granular medium will become a liquid. Current research in the field of friction in nanotribology[8] shows that Coulomb friction exists on surfaces up to a length-scale  $< 5nm$ . Therefore, a powder made of solid particles, where the atoms have a fixed neighborhood relation can be expected to behave like a granular medium for a grain size above  $5nm$ , albeit a cohesive one. In contrast, those polymer molecules which have not a fixed neighborhood relation show in nano-scale experiments no Coulomb friction characteristics, and they will therefore also not form a granular material even if the size of the molecules is considerably above  $5nm$ .

#### 4.6 Elongation effect for polygons

As in the case of ellipses, also for polygons the maximal shear stress is also decreased in comparison to more elongated particles, be it ellipses or polygons. In Fig. 15, the particles

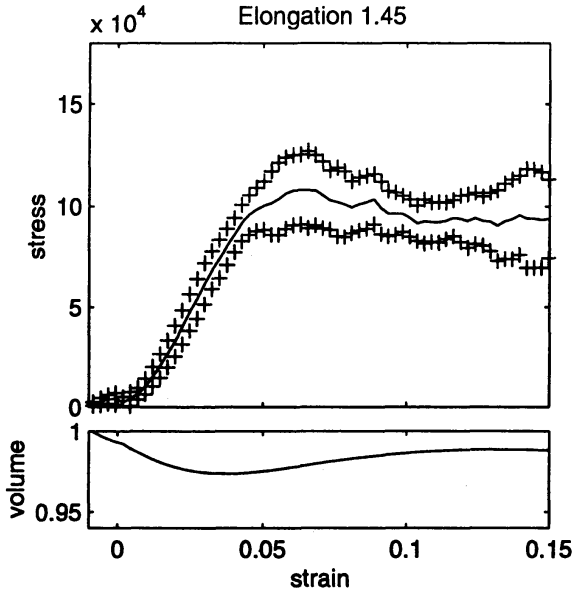


Figure 15: Ellipses with elongation 1.44 and 32 corners.

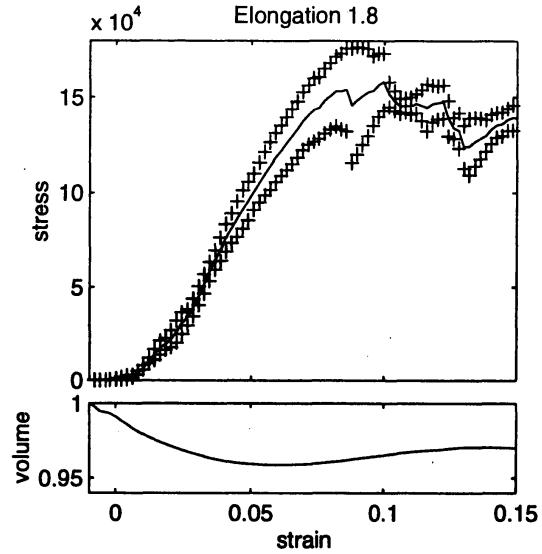


Figure 16: Stress-strain and stress-density diagram for mono-disperse polygons with 32 corners and an elongation of 1.8.

with an elongation 1.44 and 32 corners have a maximal shear stress which is between the ellipses of elongation 1.8 in Fig. 9. and the circles of Fig. 10.

### 4.7 Dispersion effect for polygons

Usually, granular media are composed of polydisperse systems, and therefore up to here we focused on the triaxial compression of polydisperse particle aggregates. Fig. 16 shows that aggregates of mono-disperse particles do not behave much different from those of polydisperse particles in Fig. 9, apart from increased fluctuations.

## 5 Pressure Distribution under heaps

### 5.1 Pressure dip and heap history

In a previous study, we found via simulations that the pressure distribution under sand heaps depends on the history[7], a result that was later found experimentally[9]. For a "wedge sequence", the construction method favored in powder technology, the pressure under heaps for non-spherical particles yield pressure minima (a "dip"), for a layered sequences, the construction history favored in

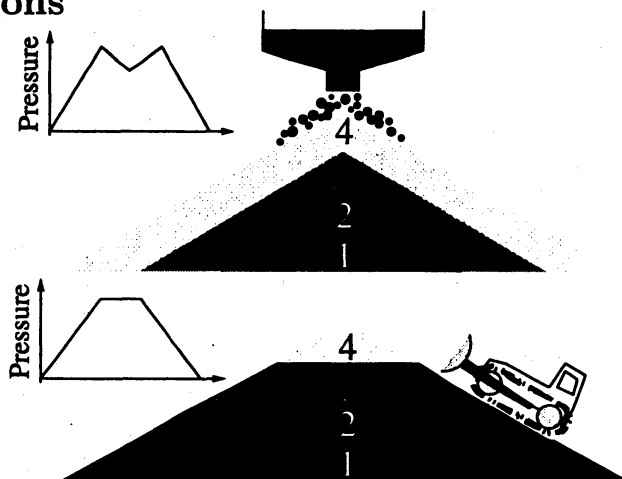


Figure 17: Schematic pressure distribution and construction histories for sand heaps for powder engineering (above) and civil engineering (below).

civil engineering, the pressure distribution in the middle of the heap remains flat. Via computer simulations, we could identify the reason for the "dip" as the density inhomogeneity resulting from the filling via the point source[10]. Such a heap density is reproduced in Fig. 18, with a density variation of about 5%. The density of a heap build in a layered sequence is given in Fig. 19. We could not find experimental density investigations for sand heaps, but the density measurements for on silo fillings[11] indicate the same density pattern for filling from a point source, and the density inhomogeneity was also found to be up to about 5 %. In our preceding research we were astonished that groups using simulations of round particles were not able to reproduce our results, inhomogeneous density and pressure dip, which we obtained for elongated particles. The reason to undertake the present study was to clear up the relation between particle shape, stress-strain and stress-density distribution.

## 5.2 Influence on the particle-shape on the pressure distributions

Experimentally, it has been found that heaps made from non-cohesive non-elongated particles show no (glass beads  $> 0.5mm$  diameter[12]) or only a vanishing (rape seed, [13], arguably slightly elongated) pressure minimum even if they are piled up in a wedge sequence, whereas small, cohesive glass beads ( $< 0.5mm$  diameter) and sand in the same experiments showed a marked pressure minimum. The apparent violation of Bagnold-scaling, where the pressure minimum depends on the size of the glass beads, can be resolved by reinterpreting cohesive non-elongated particles as elongated polydisperse particles, like molecules made up from atoms. Our simulations showed that indeed the pressure minimum developed for non-elongated particles with increasing inter-particle cohesion[14]. The reason why polydisperse round particles showed no pressure dip can be understood if the stress-strain and density-strain relations for elongated and non-elongated particles are compared. If one accepts that the pressure minimum under a heap is due to the density inhomogeneity, which allows the formation of an arch over the high-density cone in the middle of the heap, then the variation in the bulk density of up to 5 % density difference is a necessary criterion for the formation of a dip. In our triaxial compression simulations, the density variation from the uncompressed sample up to the maximal density for elongated particles is also up to 3-5 %. In contrast, for non-elongated particles, especially in the absence of static friction, the density-strain curve allows no sufficient variation of the density. Moreover, the stability of such heaps is smaller than that of heaps formed from elongated particles, so that existing density inhomogeneities are much more easily extinguished by macroscopic reordering during the pile-up process.

## 6 Conclusion:

A fundamental conclusion of our study is, that aggregates of elongated particles and particles with friction are much more stable than aggregates of round particles or particles without friction. For particulate modeling in dense granular materials, the particle shape has to be considered as fundamental parameter, like the friction coefficient. Only for realistic particle shapes and realistic coefficients of friction, the "true" stress-strain behavior of granular materials can be recovered.

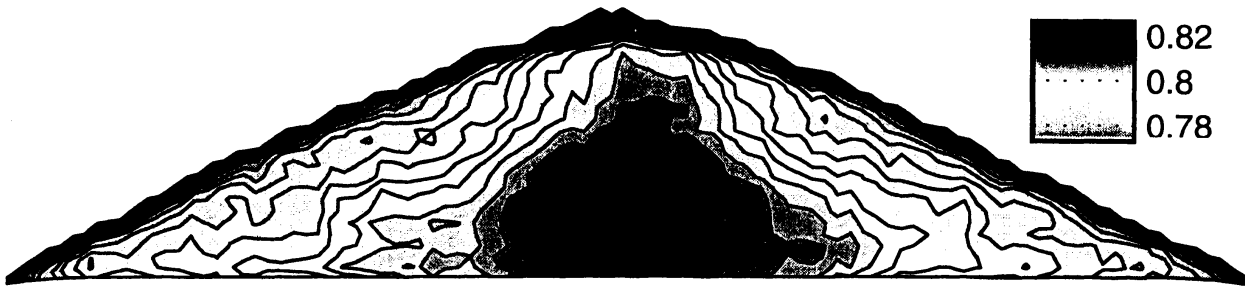


Figure 18: Density of a heap built from a point source. The high-density cone in the middle leads to the arching which caused the pressure dip.



Figure 19: Density of a heap built from a layered sequence. Due to the homogeneous density, the pressure on the base is constant under the apex.

The outcome of experiments with glass beads which do not resemble the irregular and usually elongated shape of conventional granular materials can according to our simulations be expected to show a different macroscopic behavior from that of "true" granular materials even in the most fundamental mechanical property, the mechanical strength. The value of studies of round particles for the understanding of realistic granular materials is therefore problematic.

For the formation of a pressure dip under a heap, it is necessary to maintain a density variation within the heap. This, and a higher bulk shear strength can only be obtained with elongated particles. A density variation of 5 % is must be considered significant for Rayleigh dilatancy and the pressure dip under heaps. Density measurements for granular materials piled e.g. in a layered sequence are not meaningful if the same material is piled in a wedge sequence.

For elongated particles, the stress-strain curve is not monotonous, therefore it is not possible to determine the stresses in granular aggregates from the corresponding densities. For non-elongated particles, the stress-strain curve is monotonous up to the plastic regime, but findings for granular aggregates made of non-elongated particles are not necessarily applicable to aggregates made of elongated particles.

Relating granular particles and granular bulk properties, we have shown that bulk properties of granular materials like the relative minimum of the stress-strain curve can only be obtained for elongated particles.

Some single particle properties (shape, friction coefficient) which are unimportant for dilute systems ("single-particle-problem") become important in the dense regime, where other properties which are important in the dilute regime, like normal dissipation, become

unimportant, because no dynamic collisions occur.

## References

- [1] A. Schinner, Ph.D. thesis, University of Magdeburg, 2000.
- [2] L. M. John M. Ting, Jeffrey D. Rowell, in *Proceedings on the 2nd International Conference on Discrete Element Methods (DEM)*, edited by J. R. Williams (IESL Publ., Cambridge, Mass, 1993), pp. 215–225.
- [3] F. Radjai, M. Jean, J. J. Moreau, and S. Roux, *Phys. Rev. Lett.* **77**, 274 (1996).
- [4] P. G. de Gennes, Talk in the Groupement de Recherche meeting for of dry granular Media, 22.01.1999, Paris, France.
- [5] after Stefan Diebels, personal communication.
- [6] H.-G. Matuttis, N. Ito, H. Watanabe, and K. M. Aoki, in *Powders & Grains 2001*, edited by Y.Kishino (Balkema, Rotterdam, 2001), pp. 173–176.
- [7] H.-G. Matuttis, *Granular Matter* **1**, 83 (1998).
- [8] ISSP-Workshop on Physics of Friction, 23.10-25.10.2002.
- [9] L. Vanel, D. Howell, D. Clark, R. P. Behringer, and E. Clement, *Phys. Rev. E* **60**, R5040 (1999).
- [10] A. Schinner, H.-G. Mattutis, J. Aoki, S. Takahashi, K. M. Aoki, T. Akiyama, and K. Kassner, in *Powders & Grains 2001*, edited by Y.Kishino (Balkema, Rotterdam, 2001), pp. 499–502.
- [11] J. Šmid, P. V. Xuan, and J. Thýn, *Chem. Eng. Technol.* **16**, 114 (1993).
- [12] R. Brockbank, J. M. Huntley, and R. Ball, *J. Phys. II France* **7**, 1521 (1997).
- [13] T. Jotaki and R. Moriyama, *Journal of the Society of Powder Technology, Japan* **16**, 184 (1979).
- [14] A. Schinner, H.-G. Mattutis, J. Aoki, S. Takahashi, K. M. Aoki, T. Akiyama, and K. Kassner, in *Mathematical Aspects of Complex Fluids II*, Vol. 1184 of *Kokyuroku* (Research Insitute for Mathematical Sciences, Kyoto University, 2001), pp. 123–139.